Coherent ρ^0 photoproduction in ultra-peripheral Pb-Pb collisions at √sNN = 2.76 TeV

(ALICE Collaboration) Adam, J.; ...; Antičić, Tome; ...; Erhardt, Filip; ...; Gotovac, Sven; ...; Mudnić, Eugen; ...; ...

Coherent ρ^0 photoproduction in ultra-peripheral Pb-Pb collisions at $\sqrt{s_{\mathrm{NN}}} = 2.76$ TeV

The ALICE collaboration

E-mail: ALICE-publications@cern.ch

ABSTRACT: We report the first measurement at the LHC of coherent photoproduction of ρ^0 mesons in ultra-peripheral Pb-Pb collisions. The invariant mass and transverse momentum distributions for ρ^0 production are studied in the $\pi^+\pi^-$ decay channel at mid-rapidity. The production cross section in the rapidity range $|y| < 0.5$ is found to be $\mathrm{d}\sigma/\mathrm{d}y = 425 \pm 10\,(\mathrm{stat.})\,^{+42}_{-50}\,(\mathrm{sys.})$ mb. Coherent ρ^0 production is studied with and without requirement of nuclear breakup, and the fractional yields for various breakup scenarios are presented. The results are compared with those from lower energies and with model predictions.

Contents

1 Introduction

Charged particle beams at the LHC generate an electromagnetic field which can be regarded as a beam of quasi-real photons; thus at the LHC, besides hadronic interactions, also photonuclear and photon-photon interactions occur. Collisions in which the impact parameter exceeds the sum of the radii of the incoming beam particles are called ultra-peripheral collisions (UPC). In UPC the cross section for hadronic processes is strongly suppressed, while the cross sections for two-photon and photonuclear interactions remain large. This is particularly the case for heavy ions, because the intensity of the photon flux grows with the square of the ion charge, Z. A number of reviews of UPC are available; e.g., [1, 2]. The ALICE Collaboration has previously studied exclusive photoproduction of J/ψ in ultra-peripheral Pb-Pb and p-Pb collisions [3–5].

Exclusive photoproduction of ρ^0 vector mesons, $\mathrm{Pb} + \mathrm{Pb} \rightarrow \mathrm{Pb} + \mathrm{Pb} + \rho^0$, can be described as the fluctuation of a quasi-real photon into a virtual ρ^0 vector meson, which then scatters elastically off the target nucleus. Two cases can be distinguished. When the interaction involves the complete target nucleus, the process is called coherent. In this case the target nucleus normally remains intact. If the virtual ρ^0 vector meson scatters off only one of the nucleons in the target, then the process is called incoherent and in this case the target nucleus normally breaks up, emitting neutrons at very forward rapidities. For coherent processes, the size of the lead ion restricts the mean transverse momentum of the vector meson to be about $60 \, \mathrm{MeV}/c$ corresponding to a de Broglie wavelength of the nuclear size, while it is of the order of $500 \, \mathrm{MeV}/c$ for incoherent processes.

Because of the strong electromagnetic fields in ultra-peripheral collisions of heavy ions, multiple photons may be exchanged in a single event. The additional photons can lead to excitation of the nuclei. The dominant process is the excitation to a Giant Dipole Resonance [6]. As these photonuclear processes occur on a different time scale, they are

assumed to be independent, so the probabilities factorize. The excited nucleus typically decays by the emission of neutrons at very forward rapidities. The signature of these processes is thus a ρ^0 vector meson with very low transverse momentum which may be accompanied by a few neutrons at very forward rapidities but no other particles.

Photoproduction of ρ^0 vector mesons on nuclear targets has been studied in fixed target experiments with lepton beams [7], and more recently in ultra-peripheral collisions by the STAR Collaboration at RHIC at $\sqrt{s_{NN}} = 62$ [8], 130 [9], and 200 GeV [10]. STAR has also observed coherent photoproduction of the $\rho^0(1700)$ [11].

The ρ^0 vector meson gives the dominant contribution to the hadronic structure of the photon. For proton targets, the process $\gamma + p \rightarrow \rho^0 + p$ contributes about 10% to 20% of the total $\gamma + p$ cross section, depending on energy [12]. Scaling from a nucleon target to a nuclear target is often done using the Glauber model assuming Vector Meson Dominance [13]. The large value of $\sigma(\gamma + p \rightarrow \rho^0 + p)$ means that for heavy nuclei one may reach the limit where the target appears like a black disk and the total $\rho^0 + A$ cross section approaches $2\pi R_A^2$ (R_A is the nuclear radius). The situation may, however, be more complicated for several reasons. The cross section $\sigma(\gamma + p \rightarrow \rho^0 + p)$ has contributions both from Reggeon and Pomeron exchange, and its energy dependence is therefore not monotonic. Furthermore, the nuclear medium might modify the Reggeon and Pomeron components differently. There may also be interference between the ρ and ρ' production amplitudes, and these amplitudes may be affected by the nuclear environment in a different way [14]. A detailed discussion of models for photoproduction of ρ^0 on complex nuclei based on data from fixed target experiments can be found in [13].

The cross sections measured by STAR [8–10] at RHIC were found to be about a factor two less than that predicted by the calculation of ref. [15], while in agreement with STARLIGHT [16]. The reason for the difference between these two models, which both use the Glauber model to obtain the γ-nucleus cross section, will be discussed below. The many issues associated with calculating the photonuclear ρ^0 cross section and the discrepancies between models thus call for more data. In particular, it is important to establish if the trends seen at lower energies persist at higher energies.

Moreover, the total cross section for exclusive ρ^0 production is very large at LHC energies, with the models mentioned above predicting that it could be between 50–100% of the total hadronic inelastic cross section. It could thus constitute a significant background, e.g. at the trigger level, to low multiplicity peripheral hadronic interactions and to other types of ultra-peripheral collisions. It therefore has to be well understood. The high statistics in the ρ^0 sample allows the predictions for exclusive ρ^0 production accompanied by nuclear fragmentation to be tested with good precision.

This paper presents the first measurement of the cross section for coherent photoproduction of ρ^0 vector mesons in Pb-Pb collisions at the LHC. The ρ^0 is reconstructed using the $\pi^+\pi^-$ decay channel in the rapidity range $|y| < 0.5$. The rapidity interval corresponds to a γ-nucleon center of mass energy in the range $36 \leq W_{\gamma N} \leq 59$ GeV with $\langle W_{\gamma N} \rangle = 48$ GeV, about a factor of 4 higher than in any previous measurement [10]. The cross section is measured for the cases of no neutron emission and for at least one emitted neutron. The new data presented in this paper will hopefully help to clarify some of the theoretical uncertainties mentioned above.
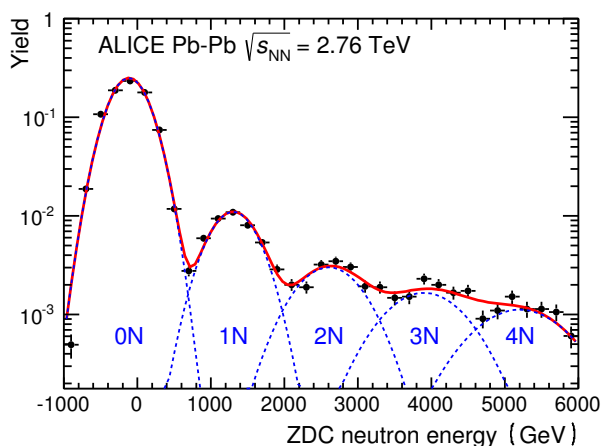
Figure 1. Energy deposit in the Zero-Degree Calorimeters. The curves correspond to Gaussian fits for 0, 1, 2, 3, or 4 neutrons entering the calorimeter. The plot is for events satisfying the requirements (i)–(vi) described in the text.

2 The ALICE experiment and the UPC trigger

A full description of the ALICE detectors and their performance can be found in [17, 18]; here, only the components relevant for this analysis will be briefly described. The Inner Tracking System (ITS) and Time Projection Chamber (TPC) are used to measure and identify the tracks of the decay products of the ρ^0 vector meson. The ITS consists of six layers of silicon detectors covering the full azimuthal angle. The two innermost layers form the Silicon Pixel Detector (SPD) with a pseudorapidity acceptance of $|\eta| < 1.4$. The SPD also provides trigger information at the lowest level. Two layers of silicon drift and two of silicon strip detectors complement the ITS, and all six layers have an acceptance of $|\eta| < 0.9$. The TPC is the main tracking detector of ALICE. It has a Ne-CO_2-N_2 gas mixture contained in a large — almost 90 m^3 — cylindrical drift detector with a central membrane at high voltage and two readout planes, composed of multi-wire proportional chambers, at the end caps. It covers the full azimuth and $|\eta| < 0.9$ for full length tracks. It also provides a measurement of the ionization energy loss, dE/dx, which allows the identification of particles. The TPC and ITS are situated inside a large solenoid magnet providing a B = 0.5 T field.

The measurement of neutrons emitted at forward rapidities is performed with a set of two neutron Zero Degree Calorimeters (ZDC) located 114 m away on each side of the interaction point. The ZDC has a 99% detection probability for neutrons with $|\eta| > 8.8$ [19]. Figure 1 illustrates the capabilities of the ZDC to separate the emission of zero, one or several neutrons at zero degrees. The sample appearing in this figure was obtained from events fulfilling the event selection described in section 3.

In addition to the SPD, this analysis uses the Time of Flight (TOF) and VZERO detectors for triggering. TOF is a large cylindrical barrel surrounding the TPC. It has 18 sectors in azimuth, each made of multigap resistive plate chambers distributed in five gas-tight modules, with a total of 152928 read-out channels and an intrinsic time resolu-

tion better than 50 ps. The pseudorapidity acceptance is the same as for the TPC. The VZERO consists of two arrays of scintillators called VZERO-A and VZERO-C, covering the pseudorapidity ranges $2.8 < \eta < 5.1$ (VZERO-A) and $-3.7 < \eta < -1.7$ (VZERO-C). Its time resolution, better than 500 ps [20], allows beam-beam collisions to be distinguished from beam-gas collisions.

The data used for this analysis were collected during the 2010 Pb-Pb run of the LHC at an energy of $\sqrt{s_{\mathrm{NN}}} = 2.76$ TeV. Two different triggers were used. At the beginning of the run, when the luminosity was low, the trigger requirement was at least two hits in the TOF detector. When the luminosity was increased the trigger selection was strengthened to improve the purity by additionally requiring at least two hits in the outer layer of the SPD, and no activity in any of the VZERO arrays.

The luminosity is determined from the cross section for triggering on at least one neutron in the ZDC detectors [19]. This cross section has been determined from a van der Meer scan [21] to be $371.4 \pm 0.6\,(\mathrm{stat.})^{+24}_{-19}\,(\mathrm{syst.})$ b [18]. The integrated luminosities for the two samples are 48^{+3}_{-2} mb^{-1} (TOF trigger only) and 214^{+14}_{-11} mb^{-1} (SPD+TOF+VZERO trigger).

3 Track and event selection

In addition to the trigger selection, the events used for the analysis are required to fulfill the following requirements:

 i) a primary vertex has to be identified within 10 cm of the nominal interaction point position, along the beam direction;

 ii) the event is required to have exactly two tracks reconstructed in the TPC and ITS satisfying the track selections discussed below;

 iii) the VZERO arrays are required to be empty (the difference between the offline and online VZERO selection will be discussed below);

 iv) the energy loss in the TPC has to be consistent with that for pions within 4 standard deviations from the Bethe-Bloch expectations, i.e., $\Delta\sigma^2_{\pi^+} + \Delta\sigma^2_{\pi^-} < 16$ (see figure 2);

 v) the track pairs used to define the coherent signal have to have a transverse momentum below $150\,\mathrm{MeV}/c$ and rapidity $|y| < 0.5$, the latter requirement being imposed to avoid edge effects;

 vi) the track pairs used to define the coherent signal are required to have tracks of opposite charge.

The background estimated from like-sign pairs ($\pi^+\pi^+$ and $\pi^-\pi^-$) is below 2% and it is subtracted from the final sample bin-by-bin in invariant mass.

The track selection requires that each track has at least 70 space points, out of a maximum of 159, in the TPC and a χ^2 per degree of freedom from the Kalman fit procedure better than 4. Each track has at least one hit in the SPD with a χ^2 per ITS hit less than
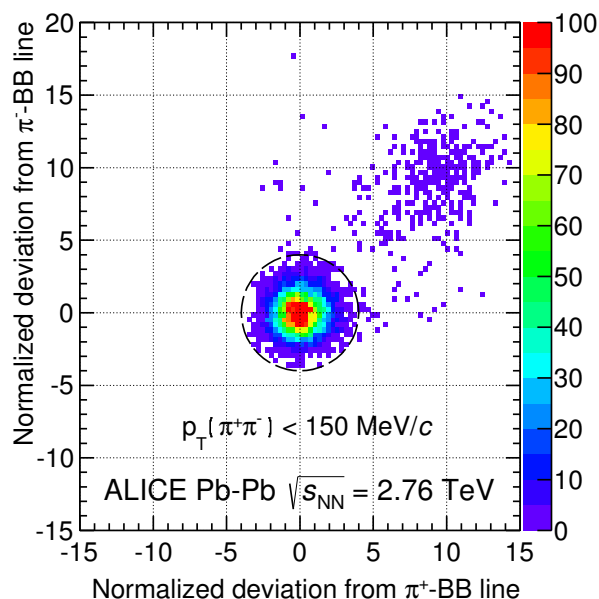
Figure 2. Identification of $\pi^{+/-}$ from the TPC dE/dx. The x– and y-axes show the deviation of the measured energy loss from the Bethe-Bloch (BB) expectations for positive and negative tracks, respectively. The scale is such that one unit corresponds to one standard deviation. The circle, corresponding to 4σ, shows the selection used. The entries in the upper right corner are from e^+e^- pairs produced in two-photon interactions. The plot is for events satisfying the requirements (i)–(iii) and (v)–(vi) described in the text.

36. The distance of closest approach between the track and the primary vertex has to be less than 2 cm along the beam direction and less than $0.0182 + 0.035/p_T^{1.01}$ cm (p_T in GeV/c) in the plane perpendicular to the beam direction. These track selection cuts are based on studies of the detector performance [18].

Three other track selections are used in order to estimate systematic errors. These differ from the default track selection described above in the following ways: (a) accepting tracks reconstructed only in the ITS in addition to combined ITS-TPC tracks satisfying the default track selection; (b) using only TPC information and accepting tracks having at least 50 space points in the TPC; (c) using the default track cuts with stronger requirements on TPC variables. The latter requirements meant that the tracks had to pass at least 120 of the 159 TPC pad rows and have a cluster in more than 80% of the crossed pad rows. For the cross section calculation, the mean of the results of the four different track selection methods is used. The systematic error related to the track selection is estimated from the deviation from the mean. This contributes $^{+3.7}_{-3.0}\%$ to the systematic error.

The momentum resolution of the ALICE central barrel tracking system [18] translates into a resolution in transverse momentum of single $\pi^+\pi^-$-pairs better than $4\,\mathrm{MeV/c}$ in the kinematic range studied here. Similarly, the resolution in invariant mass varies between $2\,\mathrm{MeV/c^2}$ ($M_{\pi\pi} = 0.4\,\mathrm{GeV/c^2}$) and $6\,\mathrm{MeV/c^2}$ ($M_{\pi\pi} = 1.5\,\mathrm{GeV/c^2}$).

The ionization energy loss for the selected tracks is shown in figure 2. The scale on both axes is in units of the number of standard deviations from the Bethe-Bloch expectation

in the TPC; in this way the dependence on track momentum is removed. Pions can be clearly identified by the 4σ circle centered on $(0, 0)$, while the events above and to the right of the pions are mostly e^+e^- pairs from $\gamma\gamma \to e^+e^-$. This figure shows that any possible contamination from kaons or protons in the sample is negligible. There could, however, be a contamination from muons from the process $\gamma\gamma \to \mu^+\mu^-$, which cannot be distinguished from pions using the energy loss. This contribution can be estimated from the number of e^+e^- pairs in the data sample, as the cross sections for $\gamma\gamma \to \mu^+\mu^-$ and $\gamma\gamma \to e^+e^-$ are about the same at midrapidity for invariant masses well above threshold. It can also be calculated from STARLIGHT [22, 23]. Both methods give an expected number of muon pairs of about 5%, which is not corrected for, but added to the systematic error. The contribution from $\gamma\gamma \to \pi^+\pi^-$ is expected to be much smaller than from $\gamma\gamma \to \mu^+\mu^-$. The $\pi^+\pi^-$ cross section is reduced by the form factor of the pion, see e.g. [24], so this contribution is not considered.

4 Data analysis

Using the event and track selection described in the previous section, the four-momenta of the two tracks are constructed and pair variables are extracted. The resulting distribution of the pair transverse momentum is shown in figure 3 for events with $0.4 \leq M_{\pi\pi} \leq 1.1\,\mathrm{GeV}/c^2$ and $|y| < 0.5$. A peak at low transverse momentum ($p_\mathrm{T} < 0.15\,\mathrm{GeV}/c$), corresponding to coherent production, is clearly seen. The distribution is compared with the corresponding distributions from STARLIGHT [16, 23] events for coherent and incoherent ρ^0 production, processed through the detector response simulation based on GEANT 3. The coherent peak is shifted to slightly lower p_T in data than that predicted by STARLIGHT. A similar trend has been observed by STAR at lower energies [25]. The shape of the coherent peak in the p_T distribution is determined by the nuclear form factor. The form factor used in STARLIGHT is consistent with what is obtained from elastic electron-nucleus scattering, which probes the charge content of the nucleus. Since the ρ^0 couples to both neutrons and protons, a possible explanation of this difference could thus be the presence of a "neutron skin". The effect, however, appears larger than what the current limit on the difference between neutron and proton radius in ^{208}Pb ($0.3\,\mathrm{fm}$) allows [26], and is thus not fully understood. Data also show a dip around $p_T = 0.12\,\mathrm{GeV}/c$, which is not present in the model. The absence of this dip in the model can be understood from the fact that in STARLIGHT the transverse momentum of the photon is considered, and this reduces the dip one would expect from the form factor of the target nucleus alone. In a Glauber calculation, the transverse momentum distribution is determined from a Fourier transform of the nuclear profile function, see e.g. [2], and the direct dependence on the form factor is only an approximation; this could also contribute to explaining the difference between STARLIGHT and data. The high-p_T tail of the distribution is very well described by the incoherent p_T spectrum from STARLIGHT.

The transverse momentum distribution for coherent production may also be parameterized as an exponential, $\mathrm{d}N/\mathrm{d}t \propto \exp(bt)$ where $t = -p_T^2$. Fitting the ALICE data to such a function gives $b = 428 \pm 6\,(\mathrm{stat.}) \pm 15\,(\mathrm{syst.})\,\mathrm{GeV}^2/c^2$. The systematic error has been
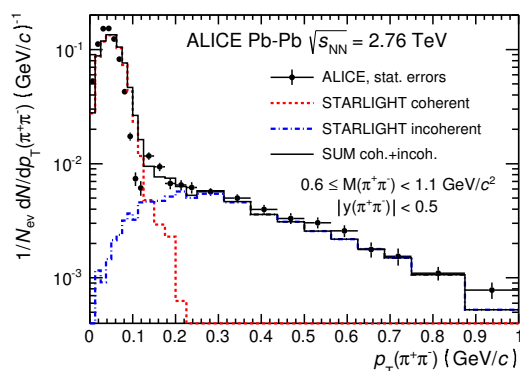
Figure 3. Transverse momentum distributions for $\pi^+\pi^-$-pairs. The dashed (red) and dash-dotted (blue) histograms show the normalized p_T distribution from STARLIGHT passed through the detector response simulation for coherent and incoherent ρ^0 production, respectively. The solid (black) histogram is the sum of the two.

obtained as the difference in slope between STARLIGHT events and STARLIGHT events processed through the full detector simulation. The ALICE result can be compared with the corresponding measurement by STAR, where $b = 388 \pm 24 \, \text{GeV}^2/c^2$ was found [10]. The STAR and ALICE results are consistent within errors if one takes into consideration that b is expected to be $\approx$4–8% larger for a lead nucleus than for a gold nucleus because of the difference in size (one expects $b \propto R^2$). The fit was performed for $|t| > 0.002 \, \text{GeV}^2/c^2$ to avoid interference effects at very low p_T [10].

The final sample of coherent $\rho^0 \to \pi^+\pi^-$ candidates is corrected for acceptance and efficiency in invariant mass bins. The event sample used to determine the corrections has uniform distributions in invariant mass, rapidity, transverse momentum, and azimuthal angle over the ranges $2m_\pi \leq M_{\pi\pi} \leq 1.5 \, \text{GeV}/c^2$, $|y| \leq 1.0$, $p_T \leq 0.15 \, \text{GeV}/c$, and $0 \leq \phi \leq 2\pi$. Using a flat distribution in transverse momentum is justified over the narrow range $p_T \leq 0.15 \, \text{GeV}/c$, where the acceptance and efficiency are constant. All models predict only a very small variation of the cross section over the range $|y| < 0.5$ (see figure 5 below) so also for rapidity a uniform input distribution is justified. The advantage of using a flat input distribution in invariant mass is to obtain sufficient statistics in the tails of the distribution. If one were to use a ρ^0-shape as input, one would need enormous statistics to cover the high and low invariant mass ranges. The ρ^0 candidates are assumed to be transversely polarized. This is expected from helicity conservation and has been confirmed by photoproduction measurements [10, 27]. This polarization translates into a $dn_\pi/d\Omega \propto \sin^2(\theta)$ angular distribution of the $\pi^+\pi^-$ decay products in their center of mass system (θ is here measured relative to the direction of flight of the ρ^0 in the γ-nucleon center of mass system). All generated samples serve as input to a full detector simulation using GEANT 3 for the propagation of particles through the detector. Selection criteria are applied in the same way as done for real events. The variation of the detector configuration during the data taking period is included in the detector response simulations. The product of acceptance and efficiency varies from about 2% at the low end of the studied invariant mass interval ($M_{\pi\pi} = 0.6 \, \text{GeV}/c^2$) to about 12% at the high end ($M_{\pi\pi} = 1.5 \, \text{GeV}/c^2$).
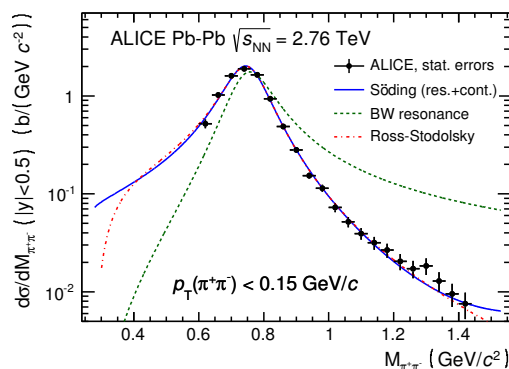
Figure 4. Invariant mass distribution for pions corrected for acceptance and efficiency. The solid (blue) curve corresponds to a fit to the Söding parameterization eq. (4.1), and the dashed (green) curve shows the resonant contribution only. The dot-dashed (red) curve shows the fit to the Ross-Stodolsky parameterization eq. (4.3). The parameters of the fit are given in the text.

The uncertainty in the trigger efficiency is obtained by comparing the measured trigger efficiency with the one in the detector response simulation in a data sample taken with a ZDC trigger [4]. The result is a trigger efficiency uncertainty of $^{+3.8}_{-9.0}\%$. In addition, a correction is applied for the trigger dead time resulting from after pulses in the TOF, originated by late particles in the event. The systematic error on this correction is estimated to be $\pm 1.3\%$.

The invariant mass distribution of the ρ^0 candidates, corrected for acceptance and efficiency and normalized by the luminosity to provide a cross section, is shown in figure 4. It is well known that the shape of the ρ^0 in photoproduction deviates from a pure Breit-Wigner resonance [7–10, 27]. Several different parameterizations exist to describe the shape, with one of the most often used being a formula due to Söding, where a continuum amplitude, B, is added to the Breit-Wigner resonance [28]:

$$\frac{\mathrm{d}\sigma}{\mathrm{d}M_{\pi\pi}} = \left| A \frac{\sqrt{M_{\pi\pi} M_{\rho^0} \Gamma(M_{\pi\pi})}}{M_{\pi\pi}^2 - M_{\rho^0}^2 + i M_{\rho^0} \Gamma(M_{\pi\pi})} + B \right|^2 . \qquad (4.1)$$

Here, A is the amplitude of the Breit-Wigner function, B is the amplitude of the direct non-resonant $\pi^+\pi^-$ production, and the mass dependent width is given by

$$\Gamma(M_{\pi\pi}) = \Gamma_{\rho^0} \frac{M_{\rho^0}}{M_{\pi\pi}} \left[\frac{M_{\pi\pi}^2 - 4m_\pi^2}{M_{\rho^0}^2 - 4m_\pi^2} \right]^{\frac{3}{2}} , \qquad (4.2)$$

with m_π the mass of the pion. Eq. 4.1 was fitted to the measured $M_{\pi\pi}$ distribution with M_{ρ^0}, Γ_{ρ^0}, A, and B as free parameters. The fit gives $M_{\rho^0} = 761.6 \pm 2.3\,(\text{stat.})^{+6.1}_{-3.0}\,(\text{syst.})\,\text{MeV}/c^2$ and $\Gamma_{\rho^0} = 150.2 \pm 5.5\,(\text{stat.})^{+12.0}_{-5.0}\,(\text{syst.})\,\text{MeV}/c^2$, in agreement with the values reported by the PDG [29]. The ratio of the non-resonant and resonant amplitudes is found to be $|B/A| = 0.50 \pm 0.04\,(\text{stat.})^{+0.10}_{-0.04}\,(\text{syst.})\,(\text{GeV}/c^2)^{-1/2}$. The systematic errors are obtained by varying the fitting method (χ^2 or log likelihood minimization), track selection (as discussed above), and fitting range.

The ratio $|B/A|$ is lower than what was found by STAR with Au targets, $|B/A| = 0.81$–$0.89 \, (\mathrm{GeV}/c^2)^{-1/2}$ for $\langle W_{\gamma N} \rangle$ in the range 7–12 GeV [8–10]. The result from ZEUS with proton targets for $\langle W_{\gamma N} \rangle$ in the range 55–90 GeV shows that $|B/A|$ varies with the γ-proton momentum tranfer [27]. The average is $|B/A| = 0.67 \pm 0.02 \, (\text{stat.}) \pm 0.04 \, (\text{syst.})$, while for momentum transfers of the same order as for coherent production $|B/A| \approx 0.8$. The lower value of $|B/A|$ observed by ALICE may indicate that the non-resonant contribution is more strongly absorbed in heavy nuclei at high energies, as had been previously suggested [30].

Other parameterizations of the ρ^0 shape are possible, and as a cross check the invariant mass distribution was also fit to a Ross-Stodolsky function [27, 31]:

$$\frac{\mathrm{d}\sigma}{\mathrm{d}M_{\pi\pi}} = f \, \left| \frac{\sqrt{M_{\pi\pi} M_{\rho^0} \Gamma(M_{\pi\pi})}}{M_{\pi\pi}^2 - M_{\rho^0}^2 + i M_{\rho^0} \Gamma(M_{\pi\pi})} \right|^2 \left(\frac{M_{\rho^0}}{M_{\pi\pi}} \right)^k \, , \tag{4.3}$$

with a slightly different definition of the mass dependent width

$$\Gamma(M_{\pi\pi}) = \Gamma_{\rho^0} \left[\frac{M_{\pi\pi}^2 - 4m_\pi^2}{M_{\rho^0}^2 - 4m_\pi^2} \right]^{\frac{3}{2}} \, . \tag{4.4}$$

As can be seen in figure 4, this parameterization also described the observed shape of the invariant mass distribution well and gave a ρ^0 mass ($M_{\rho^0} = 769.2 \pm 2.8 \, (\text{stat.})^{+8.0}_{-5.2} \, (\text{syst.}) \, \mathrm{MeV}/c^2$) and width ($\Gamma_{\rho^0} = 156.9 \pm 6.1 \, (\text{stat.})^{+17.3}_{-5.9} \, (\text{syst.}) \, \mathrm{MeV}/c^2$) consistent with the PDG values. The deviation from a pure Breit-Wigner shape is given by the parameter k, which was found to be $k = 4.7 \pm 0.2 \, (\text{stat.})^{+0.8}_{-0.6} \, (\text{syst.})$. This can be compared to the corresponding value for proton targets from ZEUS [27] and H1 [32] at HERA. ZEUS finds $k = 5.13 \pm 0.13$ averaged over all momentum transfers and $k \approx 6$ for $t = 0$, while H1 reports $k = 6.84 \pm 1.00$ averaged over all momentum transfers. The larger value of k for proton targets again indicates that the invariant mass distribution for Pb-targets deviates less from a pure Breit-Wigner resonance, as was also found using the Söding formula.

As can be seen in the lower part of figure 4, there is a hint of a resonance around $1.3 \, \mathrm{GeV}/c^2$. This may be understood from two-photon production of the $f_2(1270)$ meson followed by its decay into two pions, $\gamma + \gamma \to f_2(1270) \to \pi^+ \pi^-$. This meson is a "standard candle" in two-photon interactions with a well known $\gamma\gamma$ coupling, but it has so far not been observed in ultra-peripheral collisions because of the large background from photonuclear processes. The significance of the excess over the ρ^0 Breit-Wigner distribution is estimated to be 4^{+2}_{-1}, where the error comes from the uncertainty in the skewness of the Breit-Wigner distribution (parameter k in the Ross-Stodolsky formula).

The normalized yield of ρ^0s (N_{yield}) is obtained by integrating the resonant part of eq. (4.1) (obtained by setting $B = 0$ and taking the other parameters from the fit) from $2m_\pi$ to $1.5 \, \mathrm{GeV}/c^2$. The systematic error on the number of extracted ρ^0s is obtained by varying the fitting method (χ^2 or log likelihood minimization) and fitting range, resulting in an error of $^{+0.8}_{-1.4}\%$. The uncertainty in the track selection gives an additional error of $^{+3.7}_{-3.0}\%$ as discussed above. Both eq. (4.1) and (4.3) describe the observed shape equally well (the integrated yield differ by less than 0.5%), so no additional systematic error was added to the yield because of the choice of fitting function.

It is worth noting that the shape of the resonant contribution (shown by the dashed curve in figure 4) is quite different from the shape of the measured $\pi^+\pi^-$ invariant mass distribution. However, the integrated yield between $2m_\pi$ and $1.5\,\text{GeV}/c^2$ does not deviate by more than around 1% if the non-resonant amplitude is included in the integration.

The number of extracted ρ^0s is corrected for the following 3 contributions: incoherent events with $p_T < 0.15\,\text{GeV}/c$ (f_{incoh}), events which have one or more additional SPD tracklets (f_{SPD}), and the number of coherent ρ^0 events lost by the VZERO offline timing requirement (f_{VZERO}).

The number of incoherent events with $p_T < 0.15\,\text{GeV}/c$ is estimated in two different ways: first fitting the sum of two exponentials in p_T^2 to the p_T distributions and integrating the fitted functions over the interval chosen for the coherent selection ($p_T < 0.15\,\text{GeV}/c$), and second using the fit to the STARLIGHT templates shown in figure 3. The correction for incoherent events is found to be 5.1% in both cases with an uncertainty estimated from using different track selections of $\pm 0.7\%$.

The track selection (a) above allows one to check the events for any additional activity in the ITS, for example from tracks with low momenta, which do not reach the TPC, using SPD tracklets, defined as any combination of hits from the two SPD layers. Rejecting events with one or more extra tracklets, not associated with the two good tracks coming from the primary vertex, removes 3.0% of the events in the signal region. Since true UPC events should have no additional tracks, the extracted yield is corrected for this. In the Monte Carlo samples of coherently produced ρ^0s, the same cut removes only 0.5% of the events which is taken as the systematic error associated with this cut.

The events selected by the SPD+TOF+VZERO trigger are required to have no online signal in the VZERO detector. A similar cut is also applied offline to the events triggered by TOF only. The VZERO offline selection is further refined using the timing information. This selection has been tuned to work well for hadronic interactions, which typically have a non-zero signal in the VZERO on both sides. In the ultra-peripheral events studied here, where the VZERO is required to be empty, the offline selection is less reliable, and a coherent signal can be observed in the events with 2 tracks rejected by the offline VZERO requirement. The increase in the coherent signal when the offline VZERO selection is not used amounts to 10.0%. The systematic error of this number is obtained from the estimated contamination from hadronic events following from this looser cut. This contamination is determined from the fraction of the events which have a signal in the ZDCs, resulting in a systematic error of $^{+0.0}_{-3.1}\%$.

The corrected number of coherent ρ^0s is then obtained from

$$N_\rho^{coh} = \frac{N_{\text{yield}}}{1 + f_{\text{incoh}} + f_{\text{SPD}} + f_{\text{VZERO}}} \, , \qquad (4.5)$$

with $f_{\text{incoh}} = 0.051 \pm 0.007$, $f_{\text{SPD}} = 0.030 \pm 0.005$, and $f_{\text{VZERO}} = -0.100^{+0.031}_{-0.000}$. From this number the differential cross section is calculated as

$$\frac{\mathrm{d}\sigma}{\mathrm{d}y} = \frac{N_\rho^{coh}}{L_{\text{int}} \cdot \Delta y} \, . \qquad (4.6)$$

Variable	Systematic error
Luminosity	$^{+6.5\%}_{-5.1\%}$
Trigger efficiency	$^{+3.8\%}_{-9.0\%}$
Trigger dead time correction	$\pm1.3\%$
Signal extraction	$^{+0.8\%}_{-1.4\%}$
Track selection	$^{+3.7\%}_{-3.0\%}$
Particle ID	$^{+0.0\%}_{-5.0\%}$
Incoherent contribution	$\pm0.7\%$
SPD tracklets	$\pm0.5\%$
VZERO offline selection	$^{+0.0\%}_{-3.1\%}$
Total	$^{+9.2\%}_{-11.2\%}$

Table 1. Summary of the systematic error in the cross section calculation. The numbers are for the SPD+TOF+VZERO trigger sample. For a discussion of the TOF only trigger sample and the separation between correlated and uncorrelated errors of the two samples, see the text.

The systematic errors discussed above are summarized in table 1. They have been evaluated for the SPD+TOF+VZERO trigger sample, which contains more than 80% of the total integrated luminosity. The total error is obtained by adding the individual errors following the description in [33]. The two trigger samples, with appropriate errors, are compared as a cross check. They use different trigger combinations and were taken under quite different running conditions, with the typical hadronic minimum bias interaction rate being around 10 Hz during the early part of the run when the TOF only trigger was used and around 200 Hz during the later part of the run when the SPD+TOF+VZERO trigger was used. The correction factor for trigger dead time due to after pulses was thus very different for the two samples ($\approx$1 during the early part and $\approx$5 during the later part).

To make a comparison of the cross sections measured under the different trigger conditions, the systematic errors are separated into correlated and uncorrelated errors for the two trigger samples. The fully correlated errors are those related to luminosity, incoherent contribution, trigger efficiency, and particle identification. The fully uncorrelated errors are those related to the VZERO offline selection (different VZERO thresholds were used for the two data samples), the cut on SPD tracklets, and trigger dead time. The errors related to the signal extraction and track selection are found to be partly correlated, but are decorrelated for the comparison. This gives a cross section $\mathrm{d}\sigma/\mathrm{d}y = 466^{+25}_{-25}$ mb for the sample taken with the TOF only trigger and $\mathrm{d}\sigma/\mathrm{d}y = 414^{+14}_{-16}$ mb for the sample taken with the SPD+TOF+VZERO trigger. The error is obtained from the squared sum of the statistical and uncorrelated systematic error. The difference of 12% corresponds to 1.8 standard deviations. The final cross section is obtained as the weighted mean of the cross sections of the two samples. The weighting procedure provides a total error, including both the statistical and uncorrelated systematic components. The uncorrelated component is

separated from the total error by subtracting in quadrature the error obtained in the case when only the statistical errors are used for the weighting. The uncorrelated systematic error is then added in quadrature to the correlated systematic error to obtain the total systematic error. The final result is $\mathrm{d}\sigma/\mathrm{d}y = 425 \pm 10\,(\text{stat.})^{+42}_{-50}\,(\text{syst.})$ mb.

In addition to the ρ^0 cross section, the cross section for two-photon production of e^+e^- pairs in the range $0.6 \le M_{ee} \le 2.0\,\mathrm{GeV/c^2}$ and $|\eta_{1,2}| < 0.9$ ($\eta_{1,2}$ are the pseudorapidities of the two tracks) was measured. The analysis is similar to the one for ρ^0 but the PID requirement was modified to accept electrons rather than pions. The detector efficiency is determined using STARLIGHT events processed through the full ALICE detector simulation. The result is $\sigma(0.6 \le M_{ee} \le 2.0\,\mathrm{GeV}, |\eta_{1,2}| < 0.9) = 9.8 \pm 0.6\,(\text{stat.})^{+0.9}_{-1.2}\,(\text{syst.})$ mb, which is in good agreement with the STARLIGHT [22] prediction for the same selection in invariant mass and pseudorapidity ($\sigma = 9.7$ mb). The cross sections for the individual trigger samples are $11.8 \pm 1.6\,(\text{stat.})^{+1.1}_{-1.4}\,(\text{syst.})$ mb (TOF only trigger) and $9.4 \pm 0.7\,(\text{stat.})^{+0.9}_{-1.1}\,(\text{syst.})$ mb (SPD+TOF+VZERO trigger).

As discussed above, photoproduction of vector mesons may occur in interactions where additional photons are exchanged between the nuclei, leading to neutron emission in the forward region. These neutrons may be detected in the ALICE ZDCs. Four Gaussian distributions centered around each peak with means and variances constrained to $x_n = nx_1$ and $\sigma_n = \sqrt{n}\sigma_1$ have been fitted to the ZDC energy distribution shown in figure 1. Here, x_1 and σ_1 are the position and width of the peak corresponding to one neutron, and n is the number of neutrons. In order to separate different cases of neutron emission, the minima between the first three Gaussians are used. The minimum between zero and one-neutron emission lies at half the energy per nucleon and it is roughly three sigma away from the adjacent peaks. A given event is considered to have no neutron in the ZDC if the energy registered in the calorimeter is less than $600\,\mathrm{GeV}$, one neutron if the energy lies between $600\,\mathrm{GeV}$ and $2000\,\mathrm{GeV}$ and more than one neutron if the energy is above $2000\,\mathrm{GeV}$.

The events are divided into different groups as follows: no neutrons emitted in any direction (0n0n), at least one neutron emitted in any direction (Xn), at least one neutron emitted in one direction and no neutron emitted in the other direction (0nXn), at least one neutron emitted in both directions (XnXn).

The corrections applied in obtaining the cross section from the measured yield are independent of the ZDC signal. The fractional yield for each fragmentation selection thus reflects the relative ρ^0 production cross section. The only exception to this is the correction for the incoherent contribution (f_{incoh}), which is expected to be higher when a signal is required in the ZDCs. This correction is thus calculated for each ZDC selection separately, using the same method as described above.

5 Results and discussion

The coherent ρ^0 photoproduction cross section, $\mathrm{d}\sigma/\mathrm{d}y$, is shown and compared with model predictions in figure 5. The measured cross section is in agreement with STARLIGHT [16] and the calculation by Gonçalves and Machado (GM) [34], while the GDL (Glauber-Donnachie-Landshoff) prediction [15, 35] is about a factor of 2 higher than data. The
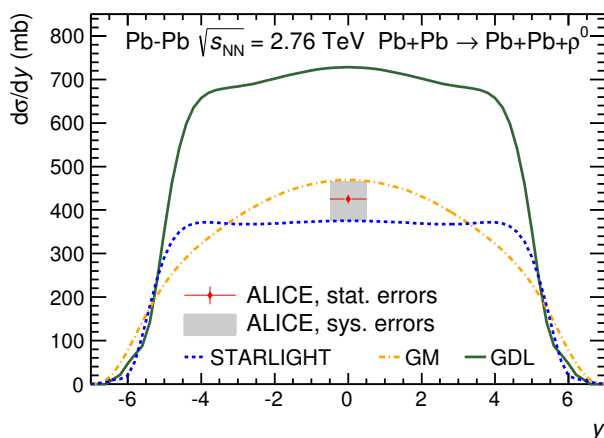
Figure 5. The cross section for coherent photoproduction of ρ^0, $d\sigma/dy$, in ultra-peripheral collisions for the three models compared with the ALICE result.

calculation by GM is based on the Color Dipole model, while STARLIGHT and GDL use the photon-proton cross section $\sigma(\gamma + \mathrm{p} \rightarrow \rho^0 + \mathrm{p})$ constrained from data as input. In STARLIGHT, the γ-nucleon cross section is given by the parameterization $\sigma = 5.0\,W_{\gamma N}^{0.20} + 26.0\,W_{\gamma N}^{-1.23}\,\mu\mathrm{b}$ ($W_{\gamma N}$ in GeV), while GDL use the Donnachie-Landshoff model [36] for the total ρN cross section. All calculations use the Glauber model to scale the cross section from γ-nucleon to γ-nucleus.

The STAR Collaboration has published the total coherent ρ^0 photoproduction cross section at three different energies [8–10]. To be able to compare the current result to those, one has to integrate $d\sigma/dy$ over the whole phase space, which can only be done using models. The extrapolation factor from $|y| < 0.5$ to all rapidities is calculated as the mean of the values obtained from the STARLIGHT (10.6) and GM (9.1) models, and the deviation of the two from the mean ($\approx 8\%$) is added to the systematic error. This gives $\sigma(\mathrm{Pb} + \mathrm{Pb} \rightarrow \mathrm{Pb} + \mathrm{Pb} + \rho^0) = 4.2 \pm 0.1(\mathrm{stat.})_{-0.6}^{+0.5}(\mathrm{syst.})$ b at $\sqrt{s_{\mathrm{NN}}} = 2.76\,\mathrm{TeV}$. The total cross section as a function of $\sqrt{s_{\mathrm{NN}}}$ is shown in figure 6, where the results from ALICE and STAR Collaborations are compared with the STARLIGHT and GDL calculations. The total cross section increases by about a factor of 5 between the top RHIC energy and $\sqrt{s_{\mathrm{NN}}} = 2.76\,\mathrm{TeV}$.

The cross section and its energy dependence is well described by STARLIGHT, while the GDL calculation overpredicts the cross section by about a factor of 2. The agreement with STARLIGHT is somewhat surprising since its Glauber calculation does not include the elastic part of the total cross section, which is included in the GDL model. It has been argued that coherent ρ^0 production off heavy nuclei may probe the onset of the Black Body Limit, in which the total ρ^0-nucleus cross section approaches $2\pi R_A^2$ at high energies [15]. The results from STAR and ALICE do not favour this picture. The cross section is instead reduced by about a factor of 2 compared with the GDL model [35], independent of energy, indicating that further work is needed to understand this process. It should be noted that none of the models in figure 5 include cross terms such as $\rho + \mathrm{N} \rightarrow \rho' + \mathrm{N}$.
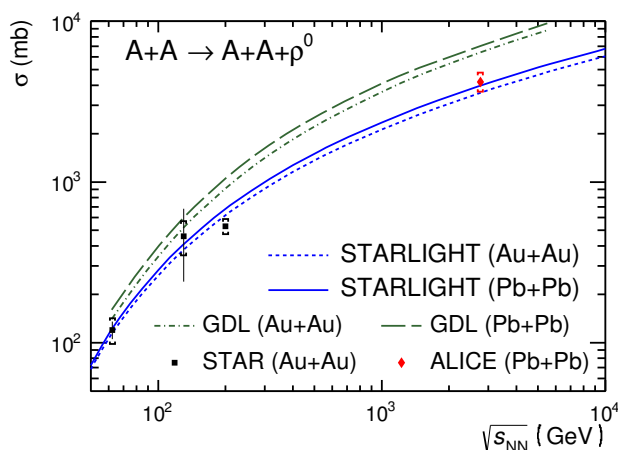
Figure 6. Excitation function for coherent and exclusive ρ^0 production. The results from ALICE and STAR [8–10] are compared with the STARLIGHT and GDL predictions for Pb-Pb and Au-Au.

The photonuclear cross section, $\sigma(\gamma + \mathrm{Pb} \to \rho^0 + \mathrm{Pb})$, in STARLIGHT is almost energy independent for $W_{\gamma N} > 10\,\mathrm{GeV}$. The increase in the Pb-Pb cross section, $\sigma(\mathrm{Pb} + \mathrm{Pb} \to \mathrm{Pb} + \mathrm{Pb} + \rho^0)$, with $\sqrt{s_{\mathrm{NN}}}$ is thus almost entirely due to the increase in the photon flux at higher collision energies.

The model by GM, although in agreement with the current result, has been criticized for using the Color Dipole model for a soft probe like the ρ^0 [35]. A recent publication shows that the calculation indeed has large uncertainties arising from the choice of ρ^0 wave function and dipole cross section [37].

The number of events satisfying the different fragmentation scenarios as well as the ratio to the total number of events are shown in table 2. The table also shows the expected fractions from the STARLIGHT [38] and GDL [35] models. These models assume that the probabilities for exchange of multiple photons in a single event factorize in impact parameter space. One should note that some of the fractions are correlated: the sum of (0n0n) and (Xn) should be 100%, and the sum of (0nXn) and (XnXn) should be equal to (Xn). This is the case within errors, but the sum is not exact, since the incoherent contribution is subtracted for each selection separately. The results in table 2 are consistent with both the STARLIGHT and GDL calculations within three standard deviations.

6 Conclusions

The first LHC measurement on coherent photoproduction of ρ^0 in Pb-Pb collisions at $\sqrt{s_{\mathrm{NN}}} = 2.76\,\mathrm{TeV}$ has been presented. Comparisons with model calculations show that the measured cross section is in agreement with the predictions by STARLIGHT [16] and Gonçalves and Machado (GM) [34], despite the idiosyncrasies in these models mentioned above. The Glauber-Donnachie-Landshoff (GDL) model [15, 35] overpredicts the cross section by about a factor of two. Comparisons with results from Au-Au collisions at RHIC energies indicate that this factor of two difference is independent of collision energy

Selection	Number of events	Fraction	STARLIGHT	GDL
All events	7293	100 %		
0n0n	6175	$84.7\pm0.4\text{(stat.)}^{+0.4}_{-1.9}\text{(syst.)}$ %	79 %	80 %
Xn	1174	$16.1\pm0.4\text{(stat.)}^{+2.2}_{-0.5}\text{(syst.)}$ %	21 %	20 %
0nXn	958	$13.1\pm0.4\text{(stat.)}^{+0.9}_{-0.3}\text{(syst.)}$ %	16 %	15 %
XnXn	231	$3.2\pm0.2\text{(stat.)}^{+0.4}_{-0.1}\text{(syst.)}$ %	5.2 %	4.5 %

Table 2. The number of events that satisfy various selections on the number of neutrons detected in the ZDCs. 0n0n corresponds to no neutrons emitted in any direction; Xn to at least one neutron emitted in any direction; 0nXn to no neutrons in one direction and at least one neutron in the other direction; XnXn to at least one neutron in both directions. For the relative yield the systematic error is estimated, as explained in the text.

in the range $\sqrt{s_{\text{NN}}} = 62.4\text{--}2760\,\text{GeV}$. In a recent preprint, it is argued that inelastic nuclear shadowing combined with the inclusion of intermediate states with higher mass in the γ-vector meson transtition could explain the discrepancy [39]. Regardless of whether this is the correct explanation or not, it indicates that non-trivial corrections to the ρ^0 photoproduction cross section may become important at high photon energies.

The relative yields for different fragmentation scenarios are found to be in agreement with predictions from the STARLIGHT and GDL models. This is important not only to confirm the assumptions in the two models but also because some experiments, e.g. PHENIX [40], have relied on a ZDC signal to trigger on ultra-peripheral collisions. To be able to relate such measurements to a photonuclear cross section, it is imperative that the probabilities for exchange of multiple photons are well understood.

The total cross section is found to be about half the total hadronic inelastic cross section. This is an increase of about a factor of 5 from Au-Au collisions at $\sqrt{s_{\text{NN}}} = 200\,\text{GeV}$, where the fraction was about 10%. If the increase of the coherent ρ^0 photoproduction cross section continues to follow STARLIGHT, one can expect it to exceed the total hadronic production cross section of heavy ions such as lead or gold at a $\sqrt{s_{\text{NN}}}$ of about 20 TeV.

Acknowledgments

References

[1] A.J. Baltz, *The physics of ultraperipheral collisions at the LHC*, *Phys. Rept.* **458** (2008) 1 [arXiv:0706.3356] [INSPIRE].

[2] C.A. Bertulani, S.R. Klein and J. Nystrand, *Physics of ultra-peripheral nuclear collisions*, *Ann. Rev. Nucl. Part. Sci.* **55** (2005) 271 [nucl-ex/0502005].

[3] ALICE collaboration, *Coherent J/ψ photoproduction in ultra-peripheral Pb-Pb collisions at $\sqrt{s_{NN}} = 2.76$ TeV*, *Phys. Lett.* **B 718** (2013) 1273 [arXiv:1209.3715] [INSPIRE].

[4] ALICE collaboration, *Charmonium and e^+e^- pair photoproduction at mid-rapidity in ultra-peripheral Pb-Pb collisions at $\sqrt{s_{NN}} = 2.76$ TeV*, *Eur. Phys. J.* **C 73** (2013) 2617 [arXiv:1305.1467] [INSPIRE].

[5] ALICE collaboration, *Exclusive J/ψ photoproduction off protons in ultra-peripheral p-Pb collisions at $\sqrt{s_{NN}} = 5.02$ TeV*, *Phys. Rev. Lett.* **113** (2014) 232504 [arXiv:1406.7819] [INSPIRE].

[6] B.L. Berman and S.C. Fultz, *Measurements of the giant dipole resonance with monoenergetic photons*, *Rev. Mod. Phys.* **47** (1975) 713 [INSPIRE].

[7] G. Mcclellan et al., *Photoproduction of neutral ρ mesons*, *Phys. Rev.* **D 4** (1971) 2683 [INSPIRE].

[8] STAR collaboration, G. Agakishiev et al., *ρ^0 photoproduction in AuAu collisions at $\sqrt{s_{NN}} = 62.4$ GeV with STAR*, *Phys. Rev.* **C 85** (2012) 014910 [arXiv:1107.4630] [INSPIRE].

[9] STAR collaboration, C. Adler et al., *Coherent ρ_0 production in ultraperipheral heavy ion collisions*, *Phys. Rev. Lett.* **89** (2002) 272302 [nucl-ex/0206004] [INSPIRE].

[10] STAR collaboration, B.I. Abelev et al., *rho0 photoproduction in ultraperipheral relativistic heavy ion collisions at $\sqrt{s_{NN}}$*, *Phys. Rev.* **C 77** (2008) 034910 [arXiv:0712.3320] [INSPIRE].

[11] STAR collaboration, B.I. Abelev et al., *Observation of $\pi^+\pi^-\pi^+\pi^-$ photoproduction in ultra-peripheral heavy ion collisions at STAR*, *Phys. Rev.* **C 81** (2010) 044901 [arXiv:0912.0604] [INSPIRE].

[12] J.A. Crittenden, *Exclusive production of neutral vector mesons at the electron-proton collider HERA*, hep-ex/9704009 [INSPIRE].

[13] T.H. Bauer, R.D. Spital, D.R. Yennie and F.M. Pipkin, *The hadronic properties of the photon in high-energy interactions*, *Rev. Mod. Phys.* **50** (1978) 261 [*Erratum ibid.* **51** (1979) 407] [INSPIRE].

[14] A. Pautz and G. Shaw, *Nuclear shadowing and ρ photoproduction*, *Phys. Rev.* **C 57** (1998) 2648 [hep-ph/9710235] [INSPIRE].

[15] L. Frankfurt, M. Strikman and M. Zhalov, *Signals for black body limit in coherent ultraperipheral heavy ion collisions*, *Phys. Lett.* **B 537** (2002) 51 [hep-ph/0204175] [INSPIRE].

[16] S. Klein and J. Nystrand, *Exclusive vector meson production in relativistic heavy ion collisions*, *Phys. Rev.* **C 60** (1999) 014903 [hep-ph/9902259] [INSPIRE].

[17] ALICE collaboration, *The ALICE experiment at the CERN LHC*, 2008 *JINST* **3** S08002 [INSPIRE].

[18] ALICE collaboration, *Performance of the ALICE Experiment at the CERN LHC*, *Int. J. Mod. Phys.* **A 29** (2014) 1430044 [arXiv:1402.4476] [ɪɴSPIRE].

[19] ALICE collaboration, *Measurement of the cross section for electromagnetic dissociation with neutron emission in Pb-Pb collisions at* $\sqrt{s_{NN}} = 2.76$ *TeV*, *Phys. Rev. Lett.* **109** (2012) 252302 [arXiv:1203.2436] [ɪɴSPIRE].

[20] ALICE collaboration, *Performance of the ALICE VZERO system*, 2013 *JINST* **8** P10016 [arXiv:1306.3130] [ɪɴSPIRE].

[21] S. van der Meer, *Calibration of the effective beam height in the ISR*, CERN-ISR-PO-68-31 (1968).

[22] A.J. Baltz, Y. Gorbunov, S.R. Klein and J. Nystrand, *Two-photon interactions with nuclear breakup in relativistic heavy ion collisions*, *Phys. Rev.* **C 80** (2009) 044902 [arXiv:0907.1214] [ɪɴSPIRE].

[23] http://starlight.hepforge.org/.

[24] M. Klusek-Gawenda and A. Szczurek, $\pi^+\pi^-$ *and* $\pi^0\pi^0$ *pair production in photon-photon and in ultraperipheral ultrarelativistic heavy ion collisions*, *Phys. Rev.* **C 87** (2013) 054908 [arXiv:1302.4204] [ɪɴSPIRE].

[25] STAR collaboration, R. Debbe, ρ *meson diffraction off Au nuclei*, *J. Phys. Conf. Ser.* **389** (2012) 012042 [arXiv:1209.0743] [ɪɴSPIRE].

[26] S. Abrahamyan et al., *Measurement of the neutron radius of 208Pb through parity-violation in electron scattering*, *Phys. Rev. Lett.* **108** (2012) 112502 [arXiv:1201.2568] [ɪɴSPIRE].

[27] ZEUS collaboration, J. Breitweg et al., *Elastic and proton dissociative* ρ^0 *photoproduction at HERA*, *Eur. Phys. J.* **C 2** (1998) 247 [hep-ex/9712020] [ɪɴSPIRE].

[28] P. Soding, *On the apparent shift of the* ρ *meson mass in photoproduction*, *Phys. Lett.* **19** (1966) 702 [ɪɴSPIRE].

[29] PARTICLE DATA GROUP collaboration, J. Beringer et al., *Review of particle physics*, *Phys. Rev.* **D 86** (2012) 010001 [ɪɴSPIRE].

[30] T. Bauer, *High-energy photoproduction of nonresonant* $\pi^+\pi^-$ *pairs and the dipion final-state interaction*, *Phys. Rev.* **D 3** (1971) 2671 [ɪɴSPIRE].

[31] M.H. Ross and L. Stodolsky, *Photon dissociation model for vector meson photoproduction*, *Phys. Rev.* **149** (1966) 1172 [ɪɴSPIRE].

[32] H1 collaboration, S. Aid et al., *Elastic photoproduction of* ρ_0 *mesons at HERA*, *Nucl. Phys.* **B 463** (1996) 3 [hep-ex/9601004] [ɪɴSPIRE].

[33] R. Barlow, *Asymmetric systematic errors*, physics/0306138 [ɪɴSPIRE].

[34] V.P. Goncalves and M.V.T. Machado, *Vector meson production in coherent hadronic interactions: an update on predictions for RHIC and LHC*, *Phys. Rev.* **C 84** (2011) 011902 [arXiv:1106.3036] [ɪɴSPIRE].

[35] V. Rebyakova, M. Strikman and M. Zhalov, *Coherent* ρ *and* J/ψ *photoproduction in ultraperipheral processes with electromagnetic dissociation of heavy ions at RHIC and LHC*, *Phys. Lett.* **B 710** (2012) 647 [arXiv:1109.0737] [ɪɴSPIRE].

[36] A. Donnachie and P.V. Landshoff, *Exclusive vector photoproduction: confirmation of Regge theory*, *Phys. Lett.* **B 478** (2000) 146 [hep-ph/9912312] [ɪɴSPIRE].

[37] G. Sampaio dos Santos and M.V.T. Machado, *Light vector meson photoproduction in hadron-hadron and nucleus-nucleus collisions at energies available at the CERN Large Hadron Collider*, *Phys. Rev.* **C 91** (2015) 025203 [arXiv:1407.4148] [INSPIRE].

[38] A.J. Baltz, S.R. Klein and J. Nystrand, *Coherent vector meson photoproduction with nuclear breakup in relativistic heavy ion collisions*, *Phys. Rev. Lett.* **89** (2002) 012301 [nucl-th/0205031] [INSPIRE].

[39] L. Frankfurt, V. Guzey, M. Strikman and M. Zhalov, *Nuclear shadowing in photoproduction of ρ mesons in ultraperipheral nucleus collisions at RHIC and the LHC*, arXiv:1506.07150 [INSPIRE].

[40] PHENIX collaboration, S. Afanasiev et al., *Photoproduction of J/ψ and of high mass e^+e^- in ultra-peripheral Au+Au collisions at $\sqrt{s} = 200\,GeV$*, *Phys. Lett.* **B 679** (2009) 321 [arXiv:0903.2041] [INSPIRE].

The ALICE collaboration

J. Adam[39] , D. Adamová[82] , M.M. Aggarwal[86] , G. Aglieri Rinella[36] , M. Agnello[110] ,
N. Agrawal[47] , Z. Ahammed[130] , S.U. Ahn[67] , I. Aimo[93 ,110] , S. Aiola[135] , M. Ajaz[16] ,
A. Akindinov[57] , S.N. Alam[130] , D. Aleksandrov[99] , B. Alessandro[110] , D. Alexandre[101] , R. Alfaro
Molina[63] , A. Alici[104 ,12] , A. Alkin[3] , J. Alme[37] , T. Alt[42] , S. Altinpinar[18] , I. Altsybeev[129] ,
C. Alves Garcia Prado[118] , C. Andrei[77] , A. Andronic[96] , V. Anguelov[92] , J. Anielski[53] ,
T. Antičić[97] , F. Antinori[107] , P. Antonioli[104] , L. Aphecetche[112] , H. Appelshäuser[52] ,
S. Arcelli[28] , N. Armesto[17] , R. Arnaldi[110] , T. Aronsson[135] , I.C. Arsene[22] , M. Arslandok[52] ,
A. Augustinus[36] , R. Averbeck[96] , M.D. Azmi[19] , M. Bach[42] , A. Badalà[106] , Y.W. Baek[43] ,
S. Bagnasco[110] , R. Bailhache[52] , R. Bala[89] , A. Baldisseri[15] , F. Baltasar Dos Santos Pedrosa[36] ,
R.C. Baral[60] , A.M. Barbano[110] , R. Barbera[29] , F. Barile[33] , G.G. Barnaföldi[134] ,
L.S. Barnby[101] , V. Barret[69] , P. Bartalini[7] , K. Barth[36] , J. Bartke[115] , E. Bartsch[52] ,
M. Basile[28] , N. Bastid[69] , S. Basu[130] , B. Bathen[53] , G. Batigne[112] , A. Batista Camejo[69] ,
B. Batyunya[65] , P.C. Batzing[22] , I.G. Bearden[79] , H. Beck[52] , C. Bedda[110] , N.K. Behera[47 ,48] ,
I. Belikov[54] , F. Bellini[28] , H. Bello Martinez[2] , R. Bellwied[120] , R. Belmont[133] ,
E. Belmont-Moreno[63] , V. Belyaev[75] , G. Bencedi[134] , S. Beole[27] , I. Berceanu[77] , A. Bercuci[77] ,
Y. Berdnikov[84] , D. Berenyi[134] , R.A. Bertens[56] , D. Berzano[36 ,27] , L. Betev[36] , A. Bhasin[89] ,
I.R. Bhat[89] , A.K. Bhati[86] , B. Bhattacharjee[44] , J. Bhom[126] , L. Bianchi[120 ,27] , N. Bianchi[71] ,
C. Bianchin[56 ,133] , J. Bielčík[39] , J. Bielčíková[82] , A. Bilandzic[79] , R. Biswas[4] , S. Biswas[78] ,
S. Bjelogrlic[56] , F. Blanco[10] , D. Blau[99] , C. Blume[52] , F. Bock[73 ,92] , A. Bogdanov[75] ,
H. Bøggild[79] , L. Boldizsár[134] , M. Bombara[40] , J. Book[52] , H. Borel[15] , A. Borissov[95] ,
M. Borri[81] , F. Bossú[64] , M. Botje[80] , E. Botta[27] , S. Böttger[51] , P. Braun-Munzinger[96] ,
M. Bregant[118] , T. Breitner[51] , T.A. Broker[52] , T.A. Browning[94] , M. Broz[39] , E.J. Brucken[45] ,
E. Bruna[110] , G.E. Bruno[33] , D. Budnikov[98] , H. Buesching[52] , S. Bufalino[110 ,36] , P. Buncic[36] ,
O. Busch[92 ,126] , Z. Buthelezi[64] , J.T. Buxton[20] , D. Caffarri[36] , X. Cai[7] , H. Caines[135] , L. Calero
Diaz[71] , A. Caliva[56] , E. Calvo Villar[102] , P. Camerini[26] , F. Carena[36] , W. Carena[36] , J. Castillo
Castellanos[15] , A.J. Castro[123] , E.A.R. Casula[25] , C. Cavicchioli[36] , C. Ceballos Sanchez[9] ,
J. Cepila[39] , P. Cerello[110] , B. Chang[121] , S. Chapeland[36] , M. Chartier[122] , J.L. Charvet[15] ,
S. Chattopadhyay[130] , S. Chattopadhyay[100] , V. Chelnokov[3] , M. Cherney[85] , C. Cheshkov[128] ,
B. Cheynis[128] , V. Chibante Barroso[36] , D.D. Chinellato[119] , P. Chochula[36] , K. Choi[95] ,
M. Chojnacki[79] , S. Choudhury[130] , P. Christakoglou[80] , C.H. Christensen[79] , P. Christiansen[34] ,
T. Chujo[126] , S.U. Chung[95] , Z. Chunhui[56] , C. Cicalo[105] , L. Cifarelli[12 ,28] , F. Cindolo[104] ,
J. Cleymans[88] , F. Colamaria[33] , D. Colella[33] , A. Collu[25] , M. Colocci[28] , G. Conesa Balbastre[70] ,
Z. Conesa del Valle[50] , M.E. Connors[135] , J.G. Contreras[39 ,11] , T.M. Cormier[83] , Y. Corrales
Morales[27] , I. Cortés Maldonado[2] , P. Cortese[32] , M.R. Cosentino[118] , F. Costa[36] , P. Crochet[69] ,
R. Cruz Albino[11] , E. Cuautle[62] , L. Cunqueiro[36] , T. Dahms[91] , A. Dainese[107] , A. Danu[61] ,
D. Das[100] , I. Das[100 ,50] , S. Das[4] , A. Dash[119] , S. Dash[47] , S. De[118] , A. De Caro[31 ,12] , G. de
Cataldo[103] , J. de Cuveland[42] , A. De Falco[25] , D. De Gruttola[12 ,31] , N. De Marco[110] , S. De
Pasquale[31] , A. Deisting[96 ,92] , A. Deloff[76] , E. Dénes[134] , G. D'Erasmo[33] , D. Di Bari[33] , A. Di
Mauro[36] , P. Di Nezza[71] , M.A. Diaz Corchero[10] , T. Dietel[88] , P. Dillenseger[52] , R. Divià[36] ,
Ø. Djuvsland[18] , A. Dobrin[56 ,80] , T. Dobrowolski[76 , i] , D. Domenicis Gimenez[118] , B. Dönigus[52] ,
O. Dordic[22] , A.K. Dubey[130] , A. Dubla[56] , L. Ducroux[128] , P. Dupieux[69] , R.J. Ehlers[135] ,
D. Elia[103] , H. Engel[51] , B. Erazmus[112 ,36] , F. Erhardt[127] , D. Eschweiler[42] , B. Espagnon[50] ,
M. Estienne[112] , S. Esumi[126] , J. Eum[95] , D. Evans[101] , S. Evdokimov[111] , G. Eyyubova[39] ,
L. Fabbietti[91] , D. Fabris[107] , J. Faivre[70] , A. Fantoni[71] , M. Fasel[73] , L. Feldkamp[53] , D. Felea[61] ,
A. Feliciello[110] , G. Feofilov[129] , J. Ferencei[82] , A. Fernández Téllez[2] , E.G. Ferreiro[17] ,
A. Ferretti[27] , A. Festanti[30] , J. Figiel[115] , M.A.S. Figueredo[122] , S. Filchagin[98] , D. Finogeev[55] ,

F.M. Fionda[103] , E.M. Fiore[33] , M.G. Fleck[92] , M. Floris[36] , S. Foertsch[64] , P. Foka[96] , S. Fokin[99] ,
E. Fragiacomo[109] , A. Francescon[36] [,30] , U. Frankenfeld[96] , U. Fuchs[36] , C. Furget[70] , A. Furs[55] ,
M. Fusco Girard[31] , J.J. Gaardhøje[79] , M. Gagliardi[27] , A.M. Gago[102] , M. Gallio[27] ,
D.R. Gangadharan[73] , P. Ganoti[87] , C. Gao[7] , C. Garabatos[96] , E. Garcia-Solis[13] , C. Gargiulo[36] ,
P. Gasik[91] , M. Germain[112] , A. Gheata[36] , M. Gheata[61] [,36] , P. Ghosh[130] , S.K. Ghosh[4] ,
P. Gianotti[71] , P. Giubellino[36] , P. Giubilato[30] , E. Gladysz-Dziadus[115] , P. Glässel[92] , A. Gomez
Ramirez[51] , P. González-Zamora[10] , S. Gorbunov[42] , L. Görlich[115] , S. Gotovac[114] , V. Grabski[63] ,
L.K. Graczykowski[132] , A. Grelli[56] , A. Grigoras[36] , C. Grigoras[36] , V. Grigoriev[75] ,
A. Grigoryan[1] , S. Grigoryan[65] , B. Grinyov[3] , N. Grion[109] , J.F. Grosse-Oetringhaus[36] ,
J.-Y. Grossiord[128] , R. Grosso[36] , F. Guber[55] , R. Guernane[70] , B. Guerzoni[28] ,
K. Gulbrandsen[79] , H. Gulkanyan[1] , T. Gunji[125] , A. Gupta[89] , R. Gupta[89] , R. Haake[53] ,
Ø. Haaland[18] , C. Hadjidakis[50] , M. Haiduc[61] , H. Hamagaki[125] , G. Hamar[134] ,
L.D. Hanratty[101] , A. Hansen[79] , J.W. Harris[135] , H. Hartmann[42] , A. Harton[13] ,
D. Hatzifotiadou[104] , S. Hayashi[125] , S.T. Heckel[52] , M. Heide[53] , H. Helstrup[37] ,
A. Herghelegiu[77] , G. Herrera Corral[11] , B.A. Hess[35] , K.F. Hetland[37] , T.E. Hilden[45] ,
H. Hillemanns[36] , B. Hippolyte[54] , P. Hristov[36] , M. Huang[18] , T.J. Humanic[20] , N. Hussain[44] ,
T. Hussain[19] , D. Hutter[42] , D.S. Hwang[21] , R. Ilkaev[98] , I. Ilkiv[76] , M. Inaba[126] , C. Ionita[36] ,
M. Ippolitov[75] [,99] , M. Irfan[19] , M. Ivanov[96] , V. Ivanov[84] , V. Izucheev[111] , P.M. Jacobs[73] ,
C. Jahnke[118] , H.J. Jang[67] , M.A. Janik[132] , P.H.S.Y. Jayarathna[120] , C. Jena[30] , S. Jena[120] ,
R.T. Jimenez Bustamante[96] , P.G. Jones[101] , H. Jung[43] , A. Jusko[101] , P. Kalinak[58] ,
A. Kalweit[36] , J. Kamin[52] , J.H. Kang[136] , V. Kaplin[75] , S. Kar[130] , A. Karasu Uysal[68] ,
O. Karavichev[55] , T. Karavicheva[55] , E. Karpechev[55] , U. Kebschull[51] , R. Keidel[137] ,
D.L.D. Keijdener[56] , M. Keil[36] , K.H. Khan[16] , M.M. Khan[19] , P. Khan[100] , S.A. Khan[130] ,
A. Khanzadeev[84] , Y. Kharlov[111] , B. Kileng[37] , B. Kim[136] , D.W. Kim[43] [,67] , D.J. Kim[121] ,
H. Kim[136] , J.S. Kim[43] , M. Kim[43] , M. Kim[136] , S. Kim[21] , T. Kim[136] , S. Kirsch[42] , I. Kisel[42] ,
S. Kiselev[57] , A. Kisiel[132] , G. Kiss[134] , J.L. Klay[6] , C. Klein[52] , J. Klein[92] , C. Klein-Bösing[53] ,
A. Kluge[36] , M.L. Knichel[92] , A.G. Knospe[116] , T. Kobayashi[126] , C. Kobdaj[113] , M. Kofarago[36] ,
T. Kollegger[42] [,96] , A. Kolojvari[129] , V. Kondratiev[129] , N. Kondratyeva[75] , E. Kondratyuk[111] ,
A. Konevskikh[55] , C. Kouzinopoulos[36] , O. Kovalenko[76] , V. Kovalenko[129] , M. Kowalski[115] ,
S. Kox[70] , G. Koyithatta Meethaleveedu[47] , J. Kral[121] , I. Králik[58] , A. Kravčáková[40] ,
M. Krelina[39] , M. Kretz[42] , M. Krivda[101] [,58] , F. Krizek[82] , E. Kryshen[36] , M. Krzewicki[96] [,42] ,
A.M. Kubera[20] , V. Kučera[82] , T. Kugathasan[36] , C. Kuhn[54] , P.G. Kuijer[80] , I. Kulakov[42] ,
J. Kumar[47] , L. Kumar[78] [,86] , P. Kurashvili[76] , A. Kurepin[55] , A.B. Kurepin[55] , A. Kuryakin[98] ,
S. Kushpil[82] , M.J. Kweon[49] , Y. Kwon[136] , S.L. La Pointe[110] , P. La Rocca[29] , C. Lagana
Fernandes[118] , I. Lakomov[36] [,50] , R. Langoy[41] , C. Lara[51] , A. Lardeux[15] , A. Lattuca[27] ,
E. Laudi[36] , R. Lea[26] , L. Leardini[92] , G.R. Lee[101] , S. Lee[136] , I. Legrand[36] , R.C. Lemmon[81] ,
V. Lenti[103] , E. Leogrande[56] , I. León Monzón[117] , M. Leoncino[27] , P. Lévai[134] , S. Li[7] [,69] ,
X. Li[14] , J. Lien[41] , R. Lietava[101] , S. Lindal[22] , V. Lindenstruth[42] , C. Lippmann[96] , M.A. Lisa[20] ,
H.M. Ljunggren[34] , D.F. Lodato[56] , P.I. Loenne[18] , V.R. Loggins[133] , V. Loginov[75] ,
C. Loizides[73] , X. Lopez[69] , E. López Torres[9] , A. Lowe[134] , P. Luettig[52] , M. Lunardon[30] ,
G. Luparello[26] , P.H.F.N.D. Luz[118] , A. Maevskaya[55] , M. Mager[36] , S. Mahajan[89] ,
S.M. Mahmood[22] , A. Maire[54] , R.D. Majka[135] , M. Malaev[84] , I. Maldonado Cervantes[62] ,
L. Malinina[65] , D. Mal'Kevich[57] , P. Malzacher[96] , A. Mamonov[98] , L. Manceau[110] , V. Manko[99] ,
F. Manso[69] , V. Manzari[103] [,36] , M. Marchisone[27] , J. Mareš[59] , G.V. Margagliotti[26] ,
A. Margotti[104] , J. Margutti[56] , A. Marín[96] , C. Markert[116] , M. Marquard[52] , N.A. Martin[96] ,
J. Martin Blanco[112] , P. Martinengo[36] , M.I. Martínez[2] , G. Martínez García[112] , M. Martinez
Pedreira[36] , Y. Martynov[3] , A. Mas[118] , S. Masciocchi[96] , M. Masera[27] , A. Masoni[105] ,
L. Massacrier[112] , A. Mastroserio[33] , H. Masui[126] , A. Matyja[115] , C. Mayer[115] , J. Mazer[123] ,

M.A. Mazzoni[108] , D. Mcdonald[120] , F. Meddi[24] , A. Menchaca-Rocha[63] , E. Meninno[31] ,
J. Mercado Pérez[92] , M. Meres[38] , Y. Miake[126] , M.M. Mieskolainen[45] , K. Mikhaylov[57,65] ,
L. Milano[36] , J. Milosevic[22,131] , L.M. Minervini[103,23] , A. Mischke[56] , A.N. Mishra[48] ,
D. Miśkowiec[96] , J. Mitra[130] , C.M. Mitu[61] , N. Mohammadi[56] , B. Mohanty[130,78] , L. Molnar[54] ,
L. Montaño Zetina[11] , E. Montes[10] , M. Morando[30] , D.A. Moreira De Godoy[112] , S. Moretto[30] ,
A. Morreale[112] , A. Morsch[36] , V. Muccifora[71] , E. Mudnic[114] , D. Mühlheim[53] , S. Muhuri[130] ,
M. Mukherjee[130] , H. Müller[36] , J.D. Mulligan[135] , M.G. Munhoz[118] , S. Murray[64] , L. Musa[36] ,
J. Musinsky[58] , B.K. Nandi[47] , R. Nania[104] , E. Nappi[103] , M.U. Naru[16] , C. Nattrass[123] ,
K. Nayak[78] , T.K. Nayak[130] , S. Nazarenko[98] , A. Nedosekin[57] , L. Nellen[62] , F. Ng[120] ,
M. Nicassio[96] , M. Niculescu[61,36] , J. Niedziela[36] , B.S. Nielsen[79] , S. Nikolaev[99] , S. Nikulin[99] ,
V. Nikulin[84] , F. Noferini[104,12] , P. Nomokonov[65] , G. Nooren[56] , J. Norman[122] , A. Nyanin[99] ,
J. Nystrand[18] , H. Oeschler[92] , S. Oh[135] , S.K. Oh[66] , A. Ohlson[36] , A. Okatan[68] , T. Okubo[46] ,
L. Olah[134] , J. Oleniacz[132] , A.C. Oliveira Da Silva[118] , M.H. Oliver[135] , J. Onderwaater[96] ,
C. Oppedisano[110] , A. Ortiz Velasquez[62] , A. Oskarsson[34] , J. Otwinowski[96,115] , K. Oyama[92] ,
M. Ozdemir[52] , Y. Pachmayer[92] , P. Pagano[31] , G. Paić[62] , C. Pajares[17] , S.K. Pal[130] , J. Pan[133] ,
A.K. Pandey[47] , D. Pant[47] , V. Papikyan[1] , G.S. Pappalardo[106] , P. Pareek[48] , W.J. Park[96] ,
S. Parmar[86] , A. Passfeld[53] , V. Paticchio[103] , R.N. Patra[130] , B. Paul[100] , T. Peitzmann[56] ,
H. Pereira Da Costa[15] , E. Pereira De Oliveira Filho[118] , D. Peresunko[75,99] , C.E. Pérez Lara[80] ,
V. Peskov[52] , Y. Pestov[5] , V. Petráček[39] , V. Petrov[111] , M. Petrovici[77] , C. Petta[29] , S. Piano[109] ,
M. Pikna[38] , P. Pillot[112] , O. Pinazza[104,36] , L. Pinsky[120] , D.B. Piyarathna[120] , M. Płoskoń[73] ,
M. Planinic[127] , J. Pluta[132] , S. Pochybova[134] , P.L.M. Podesta-Lerma[117] , M.G. Poghosyan[85] ,
B. Polichtchouk[111] , N. Poljak[127] , W. Poonsawat[113] , A. Pop[77] , S. Porteboeuf-Houssais[69] ,
J. Porter[73] , J. Pospisil[82] , S.K. Prasad[4] , R. Preghenella[36,104] , F. Prino[110] , C.A. Pruneau[133] ,
I. Pshenichnov[55] , M. Puccio[110] , G. Puddu[25] , P. Pujahari[133] , V. Punin[98] , J. Putschke[133] ,
H. Qvigstad[22] , A. Rachevski[109] , S. Raha[4] , S. Rajput[89] , J. Rak[121] , A. Rakotozafindrabe[15] ,
L. Ramello[32] , R. Raniwala[90] , S. Raniwala[90] , S.S. Räsänen[45] , B.T. Rascanu[52] , D. Rathee[86] ,
K.F. Read[123] , J.S. Real[70] , K. Redlich[76] , R.J. Reed[133] , A. Rehman[18] , P. Reichelt[52] ,
F. Reidt[92,36] , X. Ren[7] , R. Renfordt[52] , A.R. Reolon[71] , A. Reshetin[55] , F. Rettig[42] ,
J.-P. Revol[12] , K. Reygers[92] , V. Riabov[84] , R.A. Ricci[72] , T. Richert[34] , M. Richter[22] ,
P. Riedler[36] , W. Riegler[36] , F. Riggi[29] , C. Ristea[61] , A. Rivetti[110] , E. Rocco[56] , M. Rodríguez
Cahuantzi[2] , A. Rodriguez Manso[80] , K. Røed[22] , E. Rogochaya[65] , D. Rohr[42] , D. Röhrich[18] ,
R. Romita[122] , F. Ronchetti[71] , L. Ronflette[112] , P. Rosnet[69] , A. Rossi[36] , F. Roukoutakis[87] ,
A. Roy[48] , C. Roy[54] , P. Roy[100] , A.J. Rubio Montero[10] , R. Rui[26] , R. Russo[27] , E. Ryabinkin[99] ,
Y. Ryabov[84] , A. Rybicki[115] , S. Sadovsky[111] , K. Šafařík[36] , B. Sahlmuller[52] , P. Sahoo[48] ,
R. Sahoo[48] , S. Sahoo[60] , P.K. Sahu[60] , J. Saini[130] , S. Sakai[71] , M.A. Saleh[133] , C.A. Salgado[17] ,
J. Salzwedel[20] , S. Sambyal[89] , V. Samsonov[84] , X. Sanchez Castro[54] , L. Šándor[58] ,
A. Sandoval[63] , M. Sano[126] , G. Santagati[29] , D. Sarkar[130] , E. Scapparone[104] , F. Scarlassara[30] ,
R.P. Scharenberg[94] , C. Schiaua[77] , R. Schicker[92] , C. Schmidt[96] , H.R. Schmidt[35] ,
S. Schuchmann[52] , J. Schukraft[36] , M. Schulc[39] , T. Schuster[135] , Y. Schutz[112,36] , K. Schwarz[96] ,
K. Schweda[96] , G. Scioli[28] , E. Scomparin[110] , R. Scott[123] , K.S. Seeder[118] , J.E. Seger[85] ,
Y. Sekiguchi[125] , I. Selyuzhenkov[96] , K. Senosi[64] , J. Seo[95,66] , E. Serradilla[63,10] , A. Sevcenco[61] ,
A. Shabanov[55] , A. Shabetai[112] , O. Shadura[3] , R. Shahoyan[36] , A. Shangaraev[111] , A. Sharma[89] ,
N. Sharma[60,123] , K. Shigaki[46] , K. Shtejer[27,9] , Y. Sibiriak[99] , S. Siddhanta[105] ,
K.M. Sielewicz[36] , T. Siemiarczuk[76] , D. Silvermyr[83,34] , C. Silvestre[70] , G. Simatovic[127] ,
G. Simonetti[36] , R. Singaraju[130] , R. Singh[78] , S. Singha[78,130] , V. Singhal[130] , B.C. Sinha[130] ,
T. Sinha[100] , B. Sitar[38] , M. Sitta[32] , T.B. Skaali[22] , K. Skjerdal[18] , M. Slupecki[121] ,
N. Smirnov[135] , R.J.M. Snellings[56] , T.W. Snellman[121] , C. Søgaard[34] , R. Soltz[74] , J. Song[95] ,
M. Song[136] , Z. Song[7] , F. Soramel[30] , S. Sorensen[123] , M. Spacek[39] , E. Spiriti[71] ,

I. Sputowska[115] , M. Spyropoulou-Stassinaki[87] , B.K. Srivastava[94] , J. Stachel[92] , I. Stan[61] ,
G. Stefanek[76] , M. Steinpreis[20] , E. Stenlund[34] , G. Steyn[64] , J.H. Stiller[92] , D. Stocco[112] ,
P. Strmen[38] , A.A.P. Suaide[118] , T. Sugitate[46] , C. Suire[50] , M. Suleymanov[16] , R. Sultanov[57] ,
M. Šumbera[82] , T.J.M. Symons[73] , A. Szabo[38] , A. Szanto de Toledo[118 , i] , I. Szarka[38] ,
A. Szczepankiewicz[36] , M. Szymanski[132] , J. Takahashi[119] , N. Tanaka[126] , M.A. Tangaro[33] ,
J.D. Tapia Takaki[, ii,50] , A. Tarantola Peloni[52] , M. Tariq[19] , M.G. Tarzila[77] , A. Tauro[36] ,
G. Tejeda Muñoz[2] , A. Telesca[36] , K. Terasaki[125] , C. Terrevoli[30 ,25] , B. Teyssier[128] ,
J. Thäder[96 ,73] , D. Thomas[116] , R. Tieulent[128] , A.R. Timmins[120] , A. Toia[52] , S. Trogolo[110] ,
V. Trubnikov[3] , W.H. Trzaska[121] , T. Tsuji[125] , A. Tumkin[98] , R. Turrisi[107] , T.S. Tveter[22] ,
K. Ullaland[18] , A. Uras[128] , G.L. Usai[25] , A. Utrobicic[127] , M. Vajzer[82] , M. Vala[58] , L. Valencia
Palomo[69] , S. Vallero[27] , J. Van Der Maarel[56] , J.W. Van Hoorne[36] , M. van Leeuwen[56] ,
T. Vanat[82] , P. Vande Vyvre[36] , D. Varga[134] , A. Vargas[2] , M. Vargyas[121] , R. Varma[47] ,
M. Vasileiou[87] , A. Vasiliev[99] , A. Vauthier[70] , V. Vechernin[129] , A.M. Veen[56] , M. Veldhoen[56] ,
A. Velure[18] , M. Venaruzzo[72] , E. Vercellin[27] , S. Vergara Limón[2] , R. Vernet[8] , M. Verweij[133] ,
L. Vickovic[114] , G. Viesti[30 , i] , J. Viinikainen[121] , Z. Vilakazi[124] , O. Villalobos Baillie[101] ,
A. Vinogradov[99] , L. Vinogradov[129] , Y. Vinogradov[98] , T. Virgili[31] , V. Vislavicius[34] ,
Y.P. Viyogi[130] , A. Vodopyanov[65] , M.A. Völkl[92] , K. Voloshin[57] , S.A. Voloshin[133] ,
G. Volpe[36 ,134] , B. von Haller[36] , I. Vorobyev[91] , D. Vranic[96 ,36] , J. Vrláková[40] , B. Vulpescu[69] ,
A. Vyushin[98] , B. Wagner[18] , J. Wagner[96] , H. Wang[56] , M. Wang[7 ,112] , Y. Wang[92] ,
D. Watanabe[126] , M. Weber[36] , S.G. Weber[96] , J.P. Wessels[53] , U. Westerhoff[53] , J. Wiechula[35] ,
J. Wikne[22] , M. Wilde[53] , G. Wilk[76] , J. Wilkinson[92] , M.C.S. Williams[104] , B. Windelband[92] ,
M. Winn[92] , C.G. Yaldo[133] , Y. Yamaguchi[125] , H. Yang[56] , P. Yang[7] , S. Yano[46] , Z. Yin[7] ,
H. Yokoyama[126] , I.-K. Yoo[95] , V. Yurchenko[3] , I. Yushmanov[99] , A. Zaborowska[132] ,
V. Zaccolo[79] , A. Zaman[16] , C. Zampolli[104] , H.J.C. Zanoli[118] , S. Zaporozhets[65] ,
A. Zarochentsev[129] , P. Závada[59] , N. Zaviyalov[98] , H. Zbroszczyk[132] , I.S. Zgura[61] , M. Zhalov[84] ,
H. Zhang[18 ,7] , X. Zhang[73] , Y. Zhang[7] , C. Zhao[22] , N. Zhigareva[57] , D. Zhou[7] , Y. Zhou[79 ,56] ,
Z. Zhou[18] , H. Zhu[18 ,7] , J. Zhu[112 ,7] , X. Zhu[7] , A. Zichichi[12 ,28] , A. Zimmermann[92] ,
M.B. Zimmermann[53 ,36] , G. Zinovjev[3] , M. Zyzak[42]

[i] *Deceased*
[ii] *Also at: University of Kansas, Lawrence, Kansas, United States*

[1] *A.I. Alikhanyan National Science Laboratory (Yerevan Physics Institute) Foundation, Yerevan, Armenia*
[2] *Benemérita Universidad Autónoma de Puebla, Puebla, Mexico*
[3] *Bogolyubov Institute for Theoretical Physics, Kiev, Ukraine*
[4] *Bose Institute, Department of Physics and Centre for Astroparticle Physics and Space Science (CAPSS), Kolkata, India*
[5] *Budker Institute for Nuclear Physics, Novosibirsk, Russia*
[6] *California Polytechnic State University, San Luis Obispo, California, United States*
[7] *Central China Normal University, Wuhan, China*
[8] *Centre de Calcul de l'IN2P3, Villeurbanne, France*
[9] *Centro de Aplicaciones Tecnológicas y Desarrollo Nuclear (CEADEN), Havana, Cuba*
[10] *Centro de Investigaciones Energéticas Medioambientales y Tecnológicas (CIEMAT), Madrid, Spain*
[11] *Centro de Investigación y de Estudios Avanzados (CINVESTAV), Mexico City and Mérida, Mexico*
[12] *Centro Fermi - Museo Storico della Fisica e Centro Studi e Ricerche "Enrico Fermi", Rome, Italy*
[13] *Chicago State University, Chicago, Illinois, USA*
[14] *China Institute of Atomic Energy, Beijing, China*
[15] *Commissariat à l'Energie Atomique, IRFU, Saclay, France*

16   *COMSATS Institute of Information Technology (CIIT), Islamabad, Pakistan*
17   *Departamento de Física de Partículas and IGFAE, Universidad de Santiago de Compostela, Santiago de Compostela, Spain*
18   *Department of Physics and Technology, University of Bergen, Bergen, Norway*
19   *Department of Physics, Aligarh Muslim University, Aligarh, India*
20   *Department of Physics, Ohio State University, Columbus, Ohio, United States*
21   *Department of Physics, Sejong University, Seoul, South Korea*
22   *Department of Physics, University of Oslo, Oslo, Norway*
23   *Dipartimento di Elettrotecnica ed Elettronica del Politecnico, Bari, Italy*
24   *Dipartimento di Fisica dell'Università 'La Sapienza' and Sezione INFN Rome, Italy*
25   *Dipartimento di Fisica dell'Università and Sezione INFN, Cagliari, Italy*
26   *Dipartimento di Fisica dell'Università and Sezione INFN, Trieste, Italy*
27   *Dipartimento di Fisica dell'Università and Sezione INFN, Turin, Italy*
28   *Dipartimento di Fisica e Astronomia dell'Università and Sezione INFN, Bologna, Italy*
29   *Dipartimento di Fisica e Astronomia dell'Università and Sezione INFN, Catania, Italy*
30   *Dipartimento di Fisica e Astronomia dell'Università and Sezione INFN, Padova, Italy*
31   *Dipartimento di Fisica 'E.R. Caianiello' dell'Università and Gruppo Collegato INFN, Salerno, Italy*
32   *Dipartimento di Scienze e Innovazione Tecnologica dell'Università del Piemonte Orientale and Gruppo Collegato INFN, Alessandria, Italy*
33   *Dipartimento Interateneo di Fisica 'M. Merlin' and Sezione INFN, Bari, Italy*
34   *Division of Experimental High Energy Physics, University of Lund, Lund, Sweden*
35   *Eberhard Karls Universität Tübingen, Tübingen, Germany*
36   *European Organization for Nuclear Research (CERN), Geneva, Switzerland*
37   *Faculty of Engineering, Bergen University College, Bergen, Norway*
38   *Faculty of Mathematics, Physics and Informatics, Comenius University, Bratislava, Slovakia*
39   *Faculty of Nuclear Sciences and Physical Engineering, Czech Technical University in Prague, Prague, Czech Republic*
40   *Faculty of Science, P.J. Šafárik University, Košice, Slovakia*
41   *Faculty of Technology, Buskerud and Vestfold University College, Vestfold, Norway*
42   *Frankfurt Institute for Advanced Studies, Johann Wolfgang Goethe-Universität Frankfurt, Frankfurt, Germany*
43   *Gangneung-Wonju National University, Gangneung, South Korea*
44   *Gauhati University, Department of Physics, Guwahati, India*
45   *Helsinki Institute of Physics (HIP), Helsinki, Finland*
46   *Hiroshima University, Hiroshima, Japan*
47   *Indian Institute of Technology Bombay (IIT), Mumbai, India*
48   *Indian Institute of Technology Indore, Indore (IITI), India*
49   *Inha University, Incheon, South Korea*
50   *Institut de Physique Nucléaire d'Orsay (IPNO), Université Paris-Sud, CNRS-IN2P3, Orsay, France*
51   *Institut für Informatik, Johann Wolfgang Goethe-Universität Frankfurt, Frankfurt, Germany*
52   *Institut für Kernphysik, Johann Wolfgang Goethe-Universität Frankfurt, Frankfurt, Germany*
53   *Institut für Kernphysik, Westfälische Wilhelms-Universität Münster, Münster, Germany*
54   *Institut Pluridisciplinaire Hubert Curien (IPHC), Université de Strasbourg, CNRS-IN2P3, Strasbourg, France*
55   *Institute for Nuclear Research, Academy of Sciences, Moscow, Russia*
56   *Institute for Subatomic Physics of Utrecht University, Utrecht, Netherlands*
57   *Institute for Theoretical and Experimental Physics, Moscow, Russia*
58   *Institute of Experimental Physics, Slovak Academy of Sciences, Košice, Slovakia*
59   *Institute of Physics, Academy of Sciences of the Czech Republic, Prague, Czech Republic*
60   *Institute of Physics, Bhubaneswar, India*
61   *Institute of Space Science (ISS), Bucharest, Romania*
62   *Instituto de Ciencias Nucleares, Universidad Nacional Autónoma de México, Mexico City, Mexico*

63   *Instituto de Física, Universidad Nacional Autónoma de México, Mexico City, Mexico*
64   *iThemba LABS, National Research Foundation, Somerset West, South Africa*
65   *Joint Institute for Nuclear Research (JINR), Dubna, Russia*
66   *Konkuk University, Seoul, South Korea*
67   *Korea Institute of Science and Technology Information, Daejeon, South Korea*
68   *KTO Karatay University, Konya, Turkey*
69   *Laboratoire de Physique Corpusculaire (LPC), Clermont Université, Université Blaise Pascal, CNRS–IN2P3, Clermont-Ferrand, France*
70   *Laboratoire de Physique Subatomique et de Cosmologie, Université Grenoble-Alpes, CNRS-IN2P3, Grenoble, France*
71   *Laboratori Nazionali di Frascati, INFN, Frascati, Italy*
72   *Laboratori Nazionali di Legnaro, INFN, Legnaro, Italy*
73   *Lawrence Berkeley National Laboratory, Berkeley, California, United States*
74   *Lawrence Livermore National Laboratory, Livermore, California, United States*
75   *Moscow Engineering Physics Institute, Moscow, Russia*
76   *National Centre for Nuclear Studies, Warsaw, Poland*
77   *National Institute for Physics and Nuclear Engineering, Bucharest, Romania*
78   *National Institute of Science Education and Research, Bhubaneswar, India*
79   *Niels Bohr Institute, University of Copenhagen, Copenhagen, Denmark*
80   *Nikhef, National Institute for Subatomic Physics, Amsterdam, Netherlands*
81   *Nuclear Physics Group, STFC Daresbury Laboratory, Daresbury, United Kingdom*
82   *Nuclear Physics Institute, Academy of Sciences of the Czech Republic, Řež u Prahy, Czech Republic*
83   *Oak Ridge National Laboratory, Oak Ridge, Tennessee, United States*
84   *Petersburg Nuclear Physics Institute, Gatchina, Russia*
85   *Physics Department, Creighton University, Omaha, Nebraska, United States*
86   *Physics Department, Panjab University, Chandigarh, India*
87   *Physics Department, University of Athens, Athens, Greece*
88   *Physics Department, University of Cape Town, Cape Town, South Africa*
89   *Physics Department, University of Jammu, Jammu, India*
90   *Physics Department, University of Rajasthan, Jaipur, India*
91   *Physik Department, Technische Universität München, Munich, Germany*
92   *Physikalisches Institut, Ruprecht-Karls-Universität Heidelberg, Heidelberg, Germany*
93   *Politecnico di Torino, Turin, Italy*
94   *Purdue University, West Lafayette, Indiana, United States*
95   *Pusan National University, Pusan, South Korea*
96   *Research Division and ExtreMe Matter Institute EMMI, GSI Helmholtzzentrum für Schwerionenforschung, Darmstadt, Germany*
97   *Rudjer Bošković Institute, Zagreb, Croatia*
98   *Russian Federal Nuclear Center (VNIIEF), Sarov, Russia*
99   *Russian Research Centre Kurchatov Institute, Moscow, Russia*
100   *Saha Institute of Nuclear Physics, Kolkata, India*
101   *School of Physics and Astronomy, University of Birmingham, Birmingham, United Kingdom*
102   *Sección Física, Departamento de Ciencias, Pontificia Universidad Católica del Perú, Lima, Peru*
103   *Sezione INFN, Bari, Italy*
104   *Sezione INFN, Bologna, Italy*
105   *Sezione INFN, Cagliari, Italy*
106   *Sezione INFN, Catania, Italy*
107   *Sezione INFN, Padova, Italy*
108   *Sezione INFN, Rome, Italy*
109   *Sezione INFN, Trieste, Italy*
110   *Sezione INFN, Turin, Italy*
111   *SSC IHEP of NRC Kurchatov institute, Protvino, Russia*

[112] *SUBATECH, Ecole des Mines de Nantes, Université de Nantes, CNRS-IN2P3, Nantes, France*

[113] *Suranaree University of Technology, Nakhon Ratchasima, Thailand*

[114] *Technical University of Split FESB, Split, Croatia*

[115] *The Henryk Niewodniczanski Institute of Nuclear Physics, Polish Academy of Sciences, Cracow, Poland*

[116] *The University of Texas at Austin, Physics Department, Austin, Texas, USA*

[117] *Universidad Autónoma de Sinaloa, Culiacán, Mexico*

[118] *Universidade de São Paulo (USP), São Paulo, Brazil*

[119] *Universidade Estadual de Campinas (UNICAMP), Campinas, Brazil*

[120] *University of Houston, Houston, Texas, United States*

[121] *University of Jyväskylä, Jyväskylä, Finland*

[122] *University of Liverpool, Liverpool, United Kingdom*

[123] *University of Tennessee, Knoxville, Tennessee, United States*

[124] *University of the Witwatersrand, Johannesburg, South Africa*

[125] *University of Tokyo, Tokyo, Japan*

[126] *University of Tsukuba, Tsukuba, Japan*

[127] *University of Zagreb, Zagreb, Croatia*

[128] *Université de Lyon, Université Lyon 1, CNRS/IN2P3, IPN-Lyon, Villeurbanne, France*

[129] *V. Fock Institute for Physics, St. Petersburg State University, St. Petersburg, Russia*

[130] *Variable Energy Cyclotron Centre, Kolkata, India*

[131] *Vinča Institute of Nuclear Sciences, Belgrade, Serbia*

[132] *Warsaw University of Technology, Warsaw, Poland*

[133] *Wayne State University, Detroit, Michigan, United States*

[134] *Wigner Research Centre for Physics, Hungarian Academy of Sciences, Budapest, Hungary*

[135] *Yale University, New Haven, Connecticut, United States*

[136] *Yonsei University, Seoul, South Korea*

[137] *Zentrum für Technologietransfer und Telekommunikation (ZTT), Fachhochschule Worms, Worms, Germany*